Int. J. Appl. Comput. Math (2017) 3:2785–2801
DOI 10.1007/s40819-016-0260-x

ORIGINAL PAPER

Flow Behind an Exponential Shock Wave in a Rotational Axisymmetric Non-ideal Gas with Conduction and Radiation Heat Flux

G. Nath[1] · **P. K. Sahu**[1]

Published online: 26 October 2016

Abstract A self-similar model for one-dimensional unsteady adiabatic flows behind a cylindrical shock wave driven out by a piston moving with time according to an exponential law in non-ideal gas in the presence of conductive and radiative heat fluxes is discussed in a rotating atmosphere. The ambient medium is assumed to have axial, azimuthal and radial component of fluid velocities. The axial and azimuthal component of fluid velocity in the ambient medium is assumed to be varying according to exponential laws. The initial density and angular velocity of the ambient medium are taken to be constant for the existence of the similarity solutions. It is shown that increase in the parameter of non-idealness of the gas and the conductive or radiative heat transfer parameters have decaying effect on the shock wave. It is obtained that the parameter of non-idealness of the gas and heat transfer parameters have same effects on shock strength, density, pressure, axial and azimuthal component of fluid velocity and vorticity vector.

Keywords Shock wave · Self-similar flow · Rotating medium · Non-ideal gas · Conductive and radiative heat flux

Introduction

In recent years considerable attention has been given to study the interaction between gas dynamics and radiation. When the effects of radiation and conduction are taken under consideration in gas dynamics the fundamental non-linear equations are of a very complicated type and thus it is essential to determine approximations which are physically accurate and afford considerable simplifications. The problems of the interaction of radiation with gas

✉ G. Nath
gnath@mnnit.ac.in

✉ P. K. Sahu
praveensahu173@gmail.com

[1] Department of Mathematics, Motilal Nehru National Institute of Technology Allahabad, Allahabad, Uttar Pradesh 211004, India

dynamics have been studied by many authors by using the self-similar method developed by Sedov [1]. Marshak [2] studied the effect of radiation on the shock propagation by introducing the radiation diffusion approximation. He solved both the cases of constant density and constant pressure fields without invoking conditions of self similarity. Using the same mode of radiation, Elliott [3] discussed the conditions leading to self-similarity with a specified functional form of the mean free path of radiation and obtained a solution for self-similar spherical explosion. The problems of either stationary or moving radiating walls, generating shock at the head of self-similar flow-fields was discussed by Wang [4], Helliwell [5] and Nicastro [6]. Ghoneium et al. [7] obtained the self-similar solution for spherical explosions taking into account the effects of both conduction and radiation in the two limits of Rosseland radiative diffusion and Planck radiative emission.

The problem of propagation of shock waves in a rotating interplanetary atmosphere assumes special significance in the study of astrophysical phenomena. The experimental studies and astrophysical observations show that the outer atmosphere of the planets rotates because of rotation of the planets and stars. Macroscopic motion with supersonic speed occurs in an interplanetary atmosphere with rotation and shock waves are generated. Thus the rotation of planets or stars considerably affects the process taking place in their outer layers, therefore question connected with the explosions in rotating gas atmospheres are of definite astrophysical interest. Chaturani [8] obtained the solutions for the propagation of cylindrical shock wave through a gas having solid body rotation by a similarity method adopted by Sakurai [9]. Similarity solutions for the flow behind the spherical shock waves propagating in a non-uniform rotating interplanetary atmosphere with increasing energy is obtained by Nath et al. [10]. A theoretical modal of propagation of strong spherical shock waves in a self-gravitating atmosphere with radiation flux in presence of a magnetic field and considering the medium behind the shock to be rotating was studied by Ganguly and Jana [11], but they have neglected the rotation of the undisturbed medium.

Sedov [1] (see Rao and Ramana [12]) indicated that a limiting case of a self-similar flow-field with a power-law shock is the flow-field formed with an exponential shock. Rao and Ramana [12] obtained approximate analytical solutions for the problem of unsteady self-similar motion of a perfect gas displaced by a piston moving with time according to an exponential law.

Because of high pressure and density that usually occur behind a shock wave, produced by an explosion, the belief that the gas is perfect is no more valid. In recent years, several studied are performed regarding the problem of shock waves in non-ideal gases, specifically, by Anisimov and Spiner [13], Rao and Purohit [14], Vishwakarma and Nath [15], Nath [16] and many others. The popular alternative to the perfect gas might be a simplified van der Waals model. Wu and Roberts [17], Roberts and Wu [18] adopted this model to discuss the shock wave theory of sonoluminescence. In the present work, we too adopt this as our model of a non-ideal gas to find how deviations from the perfect gas can affect the self-similar solutions.

The purpose of this study is to obtain the similarity solutions for the flow behind an exponential shock wave in a rotational axisymmetric non-ideal gas with heat conduction and radiation heat flux. To obtain the similarity solution it is assumed that the density of the ambient medium is constant. The ambient medium have variable azimuthal and axial fluid velocities (Levin and Skopina [19], Nath [16,20]).

In the present work, we generalize the solution of Rao and Ramana [12] in perfect gas (the solution of Nath [27] in the case of non-ideal gas) to the case of rotational axisymmetric non-ideal gas with conductive and radiative heat fluxes, which has a variable azimuthal and axial fluid velocities (Levin and Skopina [19], Nath [20]). Here, we therefore investigate the one-dimensional unsteady self- similar adiabatic flow of a rotational axisymmetric non-ideal gas behind a shock wave driven out by cylindrical piston moving with time according to an exponential law. It is assumed that the motion of the piston obeys the exponential law (Rao and Ramanna [12], Vishwakarma and Nath [15,21])

$$r_p = C\, exp(\lambda\, t), \quad \lambda > 0, \tag{1}$$

where r_p is the radius of the piston, C and λ are dimensional constants and t is the time. 'C' represents the initial radius of the piston.

The law of piston motion (1) implies a boundary condition on the gas speed at the piston, which is required for the determination of the problem. Since we are concerned with the self-similar motions, we may assume that the shock propagation follows the exponential law

$$r_s = B\, exp(\lambda\, t), \tag{2}$$

where r_s is the radius of the shock and B is a dimensional constant which depends on the constant 'C' and the non-dimensional position of the piston (see Eq. 29).

The effects of variation of the heat transfer parameters and the parameter of the non-idealness of the gas are investigated. It is shown that the non-idealness of the gas and the conductive and radiative heat transfer parameters have decaying effect on the shock wave. It is observed that the effect of an increase in the value of radiation heat transfer parameter and conduction heat transfer parameter have similar effects on the flow variables and shock strength.

Equations of Motion and Boundary Conditions

The fundamental equations governing the one-dimensional, unsteady adiabatic and cylindrically symmetric rotational flow of a non-ideal gas with heat conduction and radiation heat flux, in Eulerian coordinates, may be expressed as (cf. Ghoneim et al. [7], Chaturani [8], Levin and Skopina [19], Nath [16,20], Gretler and Wehle [22], Vishwakarma and Nath [23])

$$\frac{\partial \rho}{\partial t} + u\frac{\partial \rho}{\partial r} + \rho\frac{\partial u}{\partial r} + \frac{u\rho}{r} = 0, \tag{3}$$

$$\frac{\partial u}{\partial t} + u\frac{\partial u}{\partial r} + \frac{1}{\rho}\frac{\partial p}{\partial r} - \frac{v^2}{r} = 0, \tag{4}$$

$$\frac{\partial v}{\partial t} + u\frac{\partial v}{\partial r} + \frac{uv}{r} = 0, \tag{5}$$

$$\frac{\partial w}{\partial t} + u\frac{\partial w}{\partial r} = 0, \tag{6}$$

$$\frac{\partial e_m}{\partial t} + u\frac{\partial e_m}{\partial r} - \frac{p}{\rho^2}\left(\frac{\partial \rho}{\partial t} + u\frac{\partial \rho}{\partial r}\right) + \frac{1}{\rho r}\frac{\partial}{\partial r}(Fr) = 0, \tag{7}$$

where r and t are independent space and time coordinates; u, v, and w are the radial, azimuthal and axial components of the fluid velocity $\overrightarrow{q}$ in the cylindrical coordinates (r, θ, z); ρ, p, e_m and F are the density, the pressure, the internal energy per unit mass and the total heat flux.

Also,

$$v = Ar, \tag{8}$$

where 'A' is the angular velocity of the medium at radial distance r from the axis of symmetry. In this case the vorticity vector

$$\vec{\zeta} = \frac{1}{2}\,Curl\,\vec{q},$$

has the components

$$\zeta_r = 0, \quad \zeta_\theta = -\frac{1}{2}\frac{\partial w}{\partial r}, \quad \zeta_z = \frac{1}{2r}\frac{\partial}{\partial r}(rv). \tag{9}$$

The total heat-flux F, which appear in the energy Eq. (7) may be decomposed as

$$F = F_c + F_R, \tag{10}$$

where F_c is conduction heat flux and F_R is radiation heat flux.

According to Fourier's law of heat conduction

$$F_c = -K\frac{\partial T}{\partial r}, \tag{11}$$

where 'K' is the coefficient of the thermal conductivity of the gas and 'T' is the absolute temperature.

Assuming local thermodynamic equilibrium and using the radiative diffusion model for an optically thick grey gas Pomroning [24], the radiative heat flux F_R may be obtain from the differential approximation of the radiation transport equation in the diffusion limit as

$$F_R = -\frac{4}{3}\left(\frac{\sigma}{\alpha_R}\right)\frac{\partial T^4}{\partial r}, \tag{12}$$

where σ is the Stefan–Boltzman constant and α_R is the Rosseland mean absorption coefficient.

The thermal conductivity 'K' and the absorption coefficient α_R of the medium are assumed to vary with temperature and density. These can be written in the form of power laws, namely (Ghoneim et al. [7], Vishwakarma and Nath [23,25])

$$K = K_0\left(\frac{T}{T_0}\right)^{\beta_c}\left(\frac{\rho}{\rho_0}\right)^{\delta_c} \quad and \quad \alpha_R = \alpha_{R_0}\left(\frac{T}{T_0}\right)^{\beta_R}\left(\frac{\rho}{\rho_0}\right)^{\delta_R}, \tag{13}$$

where the subscript '0' denotes a reference state. The exponents in the above equations should satisfy the similarity requirements if a self similar solution is sought

The system of Eqs. (3)–(7) should be supplemented with an equation of state. Most of the phenomena associated with shock wave arise in extreme conditions under which the ideal gas is not a sufficiently accurate description. To discover how deviations from the ideal gas can affect the flow behind a shock wave, we adopt a simple model. We assume that the gas obey a simplified van der Waal equation of state of the form (Nath [16], Wu and Roberts [17], Roberts and Wu [18])

$$p = \frac{\Gamma\rho T}{(1-\rho b)}; \quad e_m = C_v T = \frac{p(1-\rho b)}{\rho(\gamma-1)}, \tag{14}$$

where Γ is the gas constant, $C_v = \dfrac{\Gamma}{\gamma-1}$ is the specific heat at constant volume and γ is the ratio of specific heats. The constant b is the van der Waal excluded volume; it places a limit, $\rho_{max} = \dfrac{1}{b}$, on the density of the gas.

A cylindrical shock wave is supposed to be propagating outwards in the undisturbed rotating non-ideal gas about the axis of symmetry with constant density. In order to obtain the similarity solution, it is assumed that initial angular velocity of the medium is constant. The flow variables immediately ahead of the shock front are

$$u = u_a = 0, \tag{15}$$

$$\rho = \rho_a = constant, \tag{16}$$

$$A = A_a = constant, \tag{17}$$

$$w = w_a = w^* \; exp(\alpha\, t), \tag{18}$$

$$p_a = \rho_a \; A_a^2 \; \frac{r_s^2}{2}, \tag{19}$$

$$F = F_a = 0 \quad (Laumbach\ and\ Probstein\,[26]), \tag{20}$$

where w^* and α are constants, and the subscript 'a' refers to the conditions immediately ahead of the shock front.

Ahead of the shock, the components of the vorticity vector, therefore vary as

$$\zeta_{r_a} = 0, \tag{21}$$

$$\zeta_{\theta_a} = -\frac{w^*\alpha}{2\,\lambda\, r_s}\; exp(\alpha\, t), \tag{22}$$

$$\zeta_{z_a} = A_a. \tag{23}$$

The jump conditions are given by the conservation of mass, momentum and energy across the shock, namely,

$$\begin{aligned}
&\rho_a U = \rho_n (U - u_n),\\
&p_a + \rho_a U^2 = p_n + \rho_n (U - u_n)^2,\\
&e_{m_a} + \frac{p_a}{\rho_a} + \frac{1}{2} U^2 = e_{m_n} + \frac{p_n}{\rho_n} + \frac{1}{2}(U - u_n)^2 - \frac{F_n}{\rho_a U},\\
&v_a = v_n, \quad w_a = w_n, \quad T_a = T_n,
\end{aligned} \tag{24}$$

where the subscript 'n' denotes the conditions immediately behind the shock front, $U\left(= \frac{dr_s}{dt}\right)$ denotes the velocity of the shock front.

From Eq. (24), the conditions across the shock propagating into non-ideal gas are

$$\begin{aligned}
&\rho_n = \frac{\rho_a}{\beta}, \quad u_n = (1-\beta)U, \quad p_n = \left[(1-\beta) + \frac{1}{\gamma M^2}\right]\rho_a U^2,\\
&v_n = v_a, \quad w_n = w_a, \quad F_n = (1-\beta)\left[\frac{\overline{b}}{\gamma M^2(\beta - \overline{b})} - \frac{(1+\beta)}{2}\right]\rho_a U^3,
\end{aligned} \tag{25}$$

where $M = \left(\frac{\rho_a U^2}{\gamma p_a}\right)^{\frac{1}{2}}$ is the shock-Mach number referred to the frozen speed of sound $\left(\frac{\gamma p_a}{\rho_a}\right)^{\frac{1}{2}}$. The density ratio β $(0 < \beta < 1)$ across the shock front is given by

$$\beta = \frac{1}{\gamma M^2} + \overline{b}. \tag{26}$$

Following Levin and Skopina [19] and Nath [16,20], we obtained the jump conditions for the components of vorticity vector across the shock front as

$$\zeta_{\theta_n} = \frac{\zeta_{\theta_a}}{\beta}, \quad \zeta_{z_n} = \frac{\zeta_{z_a}}{\beta}. \tag{27}$$

Self-Similarity Transformations

We introduce $\xi = \dfrac{r}{r_s}$ as an independent variable, so that $\xi = 1$ at the shock wave and $\xi = \xi_p$ at the piston face. The field variables describing the flow pattern can be written in terms of the dimensionless functions of ξ such that (Vishwakarma and Nath [15,25], Nath [27])

$$\begin{aligned} &u = UV(\xi), \quad v = U\psi(\xi), \quad w = UW(\xi), \quad p = \rho_a U^2 P(\xi), \\ &\rho = \rho_a G(\xi), \quad F = \rho_a U^3 Q(\xi), \end{aligned} \tag{28}$$

where V, ψ, W, P, G and Q are function of ξ only.

Equations (1), (2) and (28) yields a relation between B and C in the form

$$B = \frac{C}{\xi_p}. \tag{29}$$

Using the similarity transformations (28), the system of governing Eqs. (3)–(7) can be transformed to the following system of ordinary differential equations:

$$G'\,\xi\,(V-\xi) + G\,(V'\,\xi + V) = 0, \tag{30}$$

$$(V-\xi)\,V' + \frac{P'}{G} + V - \frac{\psi^2}{\xi} = 0, \tag{31}$$

$$(V-\xi)\,\psi' + \frac{V\psi}{\xi} + \psi = 0, \tag{32}$$

$$(V-\xi)\,W' + W = 0, \tag{33}$$

$$\begin{aligned} &2\,(1-\overline{b}\,G)\,P\,G + (1-\overline{b}\,G)\,(V-\xi)\,P'\,G - (V-\xi)\,\gamma\,P\,G' \\ &\quad + \frac{(\gamma-1)\,G}{\xi}\,(Q + Q'\,\xi) = 0. \end{aligned} \tag{34}$$

Using Eqs. (11), (12) and (13) in (10), we get

$$F = -\frac{K_0}{T_0^{\beta_c}\,\rho_0^{\delta_c}}\,T^{\beta_c}\,\rho^{\delta_c}\,\frac{\partial T}{\partial r} - \frac{16\,\sigma\,T_0^{\beta_R}\,\rho_0^{\delta_R}}{3\,\alpha_{R_0}}\,T^{3-\beta_R}\,\rho^{-\delta_R}\,\frac{\partial T}{\partial r}. \tag{35}$$

Using Eqs. (14) and (28) in (35), we get

$$\begin{aligned} Q = \Bigg[&\frac{-K_0\,\lambda}{T_0^{\beta_c}\,\rho_0^{\delta_c}\,\Gamma^{\beta_c+1}}\,U^{2\beta_c-2}\,P^{\beta_c}\,(1-\overline{b}\,G)^{\beta_c}\,\rho_a^{\delta_c-1}\,G^{\delta_c-\beta_c} \\ &- \frac{16\,\sigma\,T_0^{\beta_R}\,\rho_0^{\delta_R}\,\lambda}{3\,\alpha_{R_0}\,\Gamma^{4-\beta_R}}\,U^{4-2\beta_R}\,P^{3-\beta_R}\,(1-\overline{b}\,G)^{3-\beta_R}\,\rho_a^{-1-\delta_R}\,G^{-3+\beta_R-\delta_R}\Bigg] \\ &\frac{d}{d\xi}\left(\frac{P(1-\overline{b}\,G)}{G}\right). \end{aligned} \tag{36}$$

Equation (36) shows that the similarity solution of the present problem exists only when

$$\beta_c = 1 \quad and \quad \beta_R = 2. \tag{37}$$

Therefore Eq. (36) becomes

$$Q = -X\left[\frac{(1-\overline{b}\,G)}{G}\frac{dP}{d\xi} - \frac{P}{G^2}\frac{dG}{d\xi}\right], \tag{38}$$

where $X = \left[\Gamma_c\, G^{\delta_c - 1} + \Gamma_R\, G^{-1-\delta_R}\right] P(1-\overline{b}\,G)$, Γ_c and Γ_R are the conductive and radiative non-dimensional heat transfer parameters, respectively. The parameters Γ_c and Γ_R depend on the thermal conductivity K and the mean free path of radiation $\dfrac{1}{\alpha_R}$ respectively and they are given by

$$\Gamma_c = \frac{K_0\ \lambda}{T_0\,\rho_0^{\delta_c}\,\Gamma^2}\,\rho_a^{\delta_c - 1} \quad and \quad \Gamma_R = \frac{16\,\sigma\,T_0^2\,\rho_0^{\delta_R}\ \lambda}{3\,\alpha_{R_0}\,\Gamma^2}\,\rho_a^{-1-\delta_R}.$$

Solving the set of differential Eqs. (30)–(34) and (38) for $\dfrac{dV}{d\xi}$, $\dfrac{dG}{d\xi}$, $\dfrac{dP}{d\xi}$, $\dfrac{d\psi}{d\xi}$, $\dfrac{dW}{d\xi}$ and $\dfrac{dQ}{d\xi}$, we have

$$V' = \frac{\left[(1-\overline{b}\,G)\dfrac{\psi^2 G(\xi - V)}{\xi} - (1-\overline{b}\,G)\,V\,G\,(\xi - V) - \dfrac{PV}{\xi} + \dfrac{Q\,G\,(\xi - V)}{X}\right]}{\left[P - G(V-\xi)^2(1-\overline{b}\,G)\right]}, \tag{39}$$

$$G' = \frac{G(V'\xi + V)}{\xi(\xi - V)}, \tag{40}$$

$$P' = \frac{\psi^2 G}{\xi} - (V-\xi)\,G\,V' - V\,G, \tag{41}$$

$$\psi' = \frac{\psi\,(\xi + V)}{\xi(\xi - V)}, \tag{42}$$

$$W' = \frac{W}{(\xi - V)}, \tag{43}$$

$$Q' = \frac{1}{(\gamma - 1)\xi}\Big[(V-\xi)^2(1-\overline{b}\,G)\,G\,\xi\,V' + (V-\xi)(1-\overline{b}\,G)\,G\,\xi\,V - 2\,P\,\xi\,(1-\overline{b}\,G) - (V-\xi)(1-\overline{b}\,G)\,\psi^2\,G - \gamma\,P\,\xi\,V' - \gamma\,PV - Q\,(\gamma - 1)\Big]. \tag{44}$$

Applying the similarity transformations on Eq. (9), we obtained the non-dimensional components of the vorticity vector $l_r = \dfrac{\zeta_r}{U/r_s}$, $l_\theta = \dfrac{\zeta_\theta}{U/r_s}$, $l_z = \dfrac{\zeta_z}{U/r_s}$ in the flow-filed behind the shock as

$$l_r = 0, \tag{45}$$

$$l_\theta = \frac{W}{2(V - \xi)}, \tag{46}$$

$$l_z = \frac{\psi}{(\xi - V)}. \tag{47}$$

The shock conditions (25) are transformed into

$$V(1)=(1-\beta),\quad G(1)=\frac{1}{\beta},\quad P(1)=\left[(1-\beta)+\frac{1}{\gamma M^2}\right],$$
$$\psi(1)=\frac{A_a}{\lambda},\quad W(1)=\frac{w^*}{\lambda\ B},\quad Q(1)=(1-\beta)\left[\frac{\overline{b}}{\gamma M^2(\beta-\overline{b})}-\frac{(1+\beta)}{2}\right],\tag{48}$$

where it was necessary to use $\alpha=\lambda$ to obtain the similarity solution.

In addition to the shock conditions (48), the condition to be satisfied at the piston surface is that the velocity of the fluid is equal to the velocity of the piston itself. This kinematic condition at the piston face in non-dimensional form can be written as from Eq. (28)

$$V(\xi_p)=\xi_p,\tag{49}$$

where ξ_p is the value of ξ at the piston.

For an isentropic change of state of the non-ideal gas, we may calculate the sound speed in non-ideal gas for a given b as follows

$$a=\left(\frac{\partial p}{\partial\rho}\right)_S^{\frac{1}{2}}=\left[\frac{\gamma\ p}{\rho\,(1-b\rho)}\right]^{\frac{1}{2}},\tag{50}$$

where the subscript 'S' refers to the process of constant entropy. In addition, the isothermal speed of sound may also play a role when thermal radiation is taken into account. The isothermal sound speed in non-ideal gas is

$$a_{isoth}=\left(\frac{\partial p}{\partial\rho}\right)_T^{\frac{1}{2}}=\left[\frac{p}{\rho\,(1-b\rho)}\right]^{\frac{1}{2}},\tag{51}$$

where the subscript 'T' refers to the process of constant temperature.

By using Eq. (28) the expression for reduce isothermal speed of sound (51) becomes

$$\frac{a_{isoth}}{U}=\left[\frac{P}{G\,(1-\overline{b}\,G)}\right]^{\frac{1}{2}}.\tag{52}$$

The adiabatic compressibility of non-ideal gas may be calculated as (c.f. Moelwyn-Hughes [28], Nath [27])

$$C_{adi}=\frac{1}{\rho}\left(\frac{\partial p}{\partial\rho}\right)_S=\frac{1}{\rho\,a^2}=\left[\frac{(1-b\rho)}{\gamma\ p}\right].\tag{53}$$

By using Eq. (28) in Eq. (53), we obtain the expression for the adiabatic compressibility C_{adi} as

$$C_{adi}\ \rho_a\,U^2=\frac{(1-\overline{b}\,G)}{\gamma\ P}.\tag{54}$$

The total energy of the disturbance is given by

$$E=2\pi\int_{r_p}^{r_s}\rho\left[\frac{1}{2}\left(u^2+v^2+w^2\right)+e_m\right]rdr.\tag{55}$$

Applying the similarity transformations (28) and equation (14) to the relation (55), we have

$$E=2\pi\rho_a\overset{2}{\lambda}r_s^4\int_{\xi_p}^{1}\left[\frac{1}{2}\,G\left(V^2+\psi^2+W^2\right)+\frac{P(1-\overline{b}\,G)}{(\gamma-1)}\right]\xi d\xi.\tag{56}$$

Hence, the total energy of the shock wave is not constant and varies as r_s^4. The increase in the total energy may be achieved by the pressure exerted on the fluid by the piston. The situation very much of the same kind may prevail in the formation of cylindrical spark channel from exploding wires. In addition, in the usual cases of spark break down, time dependent energy input is a more realistic assumption than instantaneous energy input. (Vishwakarma and Nath [25], Freeman and Craggs [29]).

Normalizing the variables u, v, w, p, ρ and F with their respective values at the shock front, we obtain

$$\frac{u}{u_n} = \frac{V(\xi)}{V(1)}, \quad \frac{v}{v_n} = \frac{\psi\xi)}{\psi(1)}, \quad \frac{w}{w_n} = \frac{W(\xi)}{W(1)}, \quad \frac{p}{p_n} = \frac{P(\xi)}{P(1)},$$
$$\frac{\rho}{\rho_n} = \frac{G(\xi)}{G(1)}, \quad \frac{F}{F_n} = \frac{Q(\xi)}{Q(1)}. \tag{57}$$

Because of the dependence of the boundary conditions (48) and Eqs. (39)–(44) on the parameter of non-idealness of the gas $\overline{b}(= b\,\rho_a)$, shock-Mach number M, and heat transfer parameters Γ_c and Γ_R, the similarity solutions exist only when $\overline{b}$, M, Γ_c and Γ_R are constants. Therefore, for existence of similarity solutions it is necessary to take the initial density ρ_a to be a constant.

Results and Discussion

The set of differential Eqs. (39)–(44) have been integrated numerically with the boundary conditions (48) and (49) to obtain the distributions of the flow variables in the flow-field behind the shock front by the fourth order Runge–Kutta method. For the purpose of numerical integration, the values of the physical parameters are taken to be (Ghoneim et al. [7], Vishwakarma and Nath [15,23,25], Nath [27]) $\gamma = 1.4$; $M = 5$; $\delta_c = 1$; $\delta_R = 2$; $\overline{b} = 0, 0.01, 0.025, 0.05$; $\Gamma_c = 1, 1.5, 2, 3, 3.5, 10, \infty$; $\Gamma_R = 1, 10, 1000, 5000, 10000, 15000, \infty$. The value $\overline{b} = 0$ corresponds to the perfect gas case. The set of values $\delta_c = 1,\ \delta_R = 2$ is the representative of the case of high-temperature, low-density medium (Ghoneim et al. [7]). Also, the set of values $\Gamma_c = 3,\ \Gamma_R = 10$ (taken in Fig. 2a–j) is the representative of the case in which there is heat transfer by both the conduction and radiative diffusion.

Figures 1a–j and 2a–j show the variation of the reduced flow variables $\frac{u}{u_n}$, $\frac{v}{v_n}$, $\frac{w}{w_n}$, $\frac{\rho}{\rho_n}$, $\frac{p}{p_n}$, $\frac{F}{F_n}$, the non-dimensional azimuthal component of vorticity vector l_θ, the non-dimensional axial component of vorticity vector l_z, reduced isothermal speed of sound $\frac{a_{isoth}}{U}$ and the adiabatic compressibility $C_{adi}\,\rho_a\,U^2$ against the similarity variable ξ at various values of the parameters $\overline{b}$, Γ_c and Γ_R respectively.

These figures show that the radial component of fluid velocity $\frac{u}{u_n}$, the density $\frac{\rho}{\rho_n}$, the pressure $\frac{p}{p_n}$, the axial component of vorticity vector l_z and isothermal speed of sound $\frac{a_{isoth}}{U}$ increases, but the azimuthal component of fluid velocity $\frac{v}{v_n}$, axial component of fluid velocity $\frac{w}{w_n}$, the azimuthal component of vorticity vector l_θ and the adiabatic compressibility

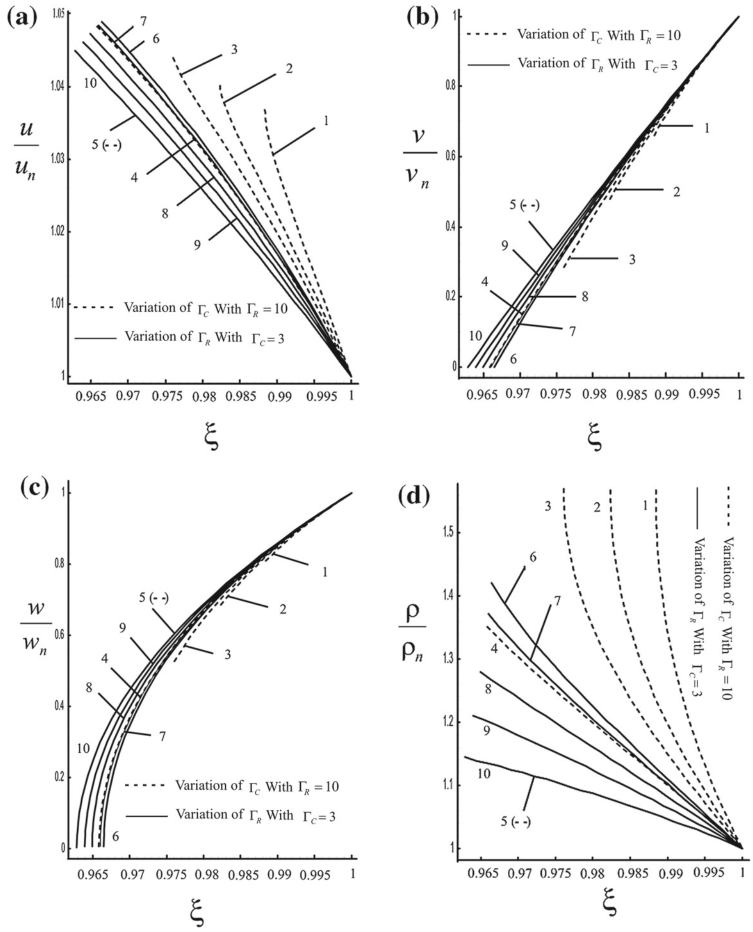

Fig. 1 Variation of the reduced flow variables in the region behind the shock front for $\overline{b} = 0.05$: **a** radial component of fluid velocity $\frac{u}{u_n}$, **b** azimuthal component of fluid velocity $\frac{v}{v_n}$, **c** axial component of fluid velocity $\frac{w}{w_n}$, **d** density $\frac{\rho}{\rho_n}$, **e** pressure $\frac{p}{p_n}$, **f** total heat flux $\frac{F}{F_n}$, **g** non-dimensional azimuthal component of vorticity vector l_θ, **h** non-dimensional axial component of vorticity vector l_z, **i** isothermal speed of sound $\frac{a_{isoth}}{U}$, **j** adiabatic compressibility $C_{adi}\,\rho_a\,U^2$: *1* $\Gamma_c = 1$, $\Gamma_R = 10$; *2* $\Gamma_c = 1.5$, $\Gamma_R = 10$; *3* $\Gamma_c = 2$, $\Gamma_R = 10$; *4* $\Gamma_c = 3.5$, $\Gamma_R = 10$; *5* $\Gamma_c = \infty$, $\Gamma_R = 10$; *6* $\Gamma_R = 1$, $\Gamma_c = 3$; *7* $\Gamma_R = 1000$, $\Gamma_c = 3$; *8* $\Gamma_R = 5000$, $\Gamma_c = 3$; *9* $\Gamma_R = 15{,}000$, $\Gamma_c = 3$; *10* $\Gamma_R = \infty$, $\Gamma_c = 3$

$C_{adi}\,\rho_a\,U^2$ decreases as we move from the shock front to the piston ingeneral (see Figs. 1a–j, 2a–j).

Flow variables $\frac{u}{u_n}$, $\frac{\rho}{\rho_n}$, $\frac{p}{p_n}$ and the axial component of vorticity vector l_z have higher values at the piston than at the shock front. In fact, since the total energy increases with time, the velocity of the piston is higher than the radial fluid velocity behind the shock front. This fact can be seen from the Table 3 which displays that $\xi_p \left(= \frac{u_p}{U}\right)$ is greater than

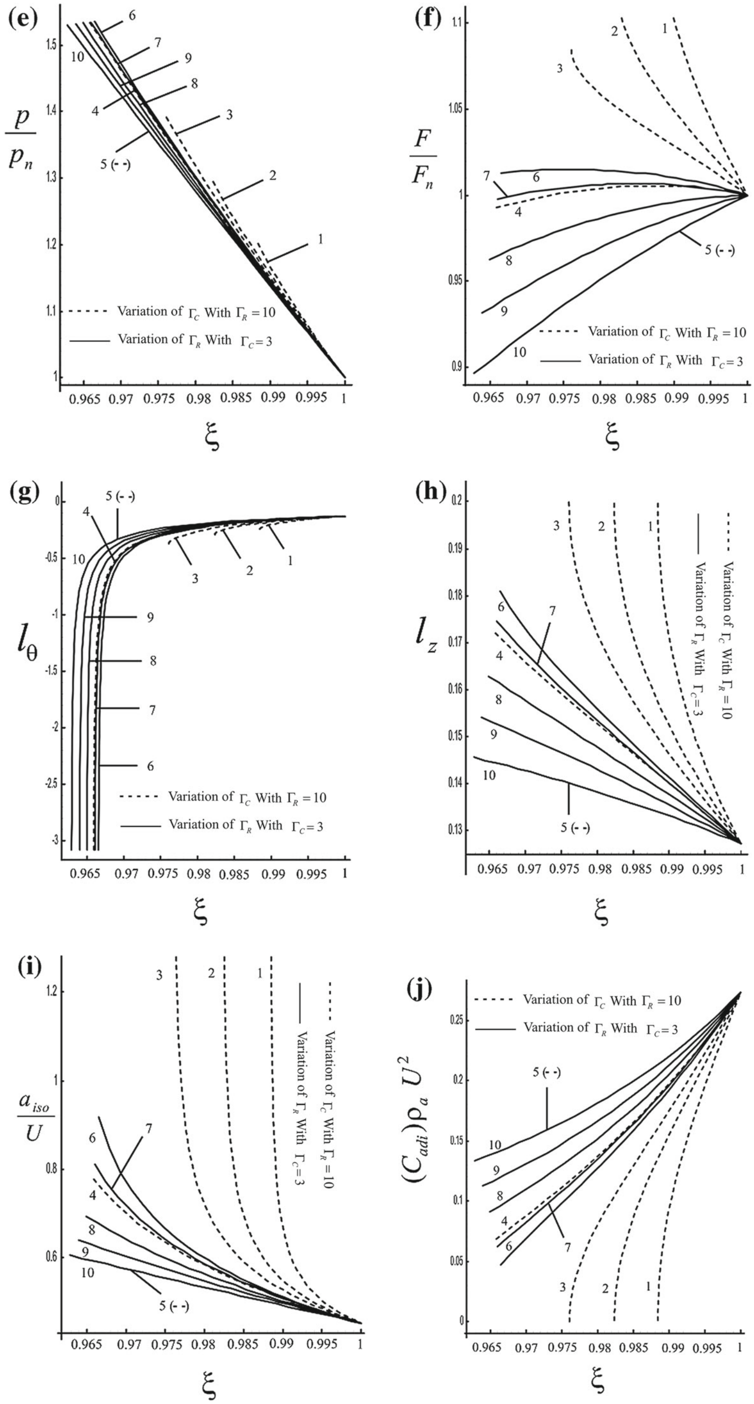

Fig. 1 continued

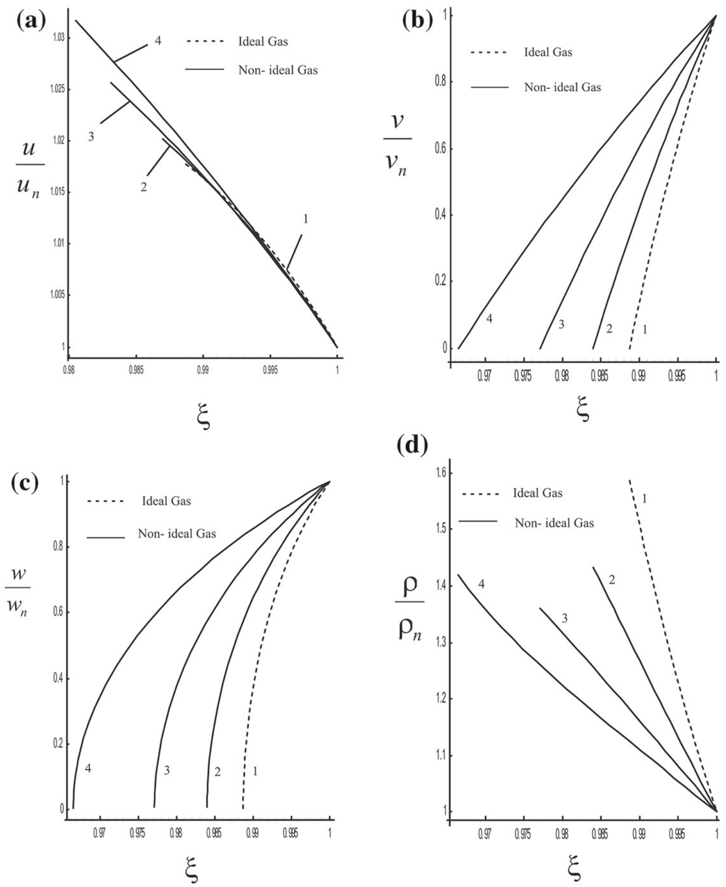

Fig. 2 Variation of the reduced flow variables in the region behind the shock front for $\Gamma_c = 3$ and $\Gamma_R = 10$: **a** radial component of fluid velocity $\frac{u}{u_n}$, **b** azimuthal component of fluid velocity $\frac{v}{v_n}$, **c** axial component of fluid velocity $\frac{w}{w_n}$, **d** density $\frac{\rho}{\rho_n}$, **e** pressure $\frac{p}{p_n}$, **f** total heat flux $\frac{F}{F_n}$, **g** non-dimensional azimuthal component of vorticity vector l_θ, **h** non-dimensional axial component of vorticity vector l_z, **i** isothermal speed of sound $\frac{a_{isoth}}{U}$, **j** adiabatic compressibility $C_{adi}\,\rho_a\,U^2$: *1* $\overline{b} = 0$; *2* $\overline{b} = 0.01$; *3* $\overline{b} = 0.025$; *4* $\overline{b} = 0.05$

$1 - \beta \left(= \frac{u_n}{U}\right)$. Therefore, most of the mass is concentrated near the piston than at the shock front (see Figs. 1a, d, e, h, 2a, d, e, h).

Figure 1j shows that the adiabatic compressibility $C_{adi}\,\rho_a\,U^2$ decreases rapidly near the piston for lower values of Γ_c, whereas it decreases in the whole flow field as we move from the shock front to the piston for higher values of Γ_c or for all values of Γ_R. In fact, when Γ_c is small the temperature near the piston increases rapidly due to absorption of energy. This rise in temperature can be seen through curves 1–3 in Fig. 1i as the isothermal speed of sound $\frac{a_{isoth}}{U}$ is proportional to the square root of the temperature (see Eq. 52). Since the adiabatic compressibility $C_{adi}\,\rho_a\,U^2$ is inversely proportional to temperature (see Eq. 54), this rise in temperature causes the adiabatic compressibility to attain a minimum near the piston (curves 1–3 in Fig. 1j).

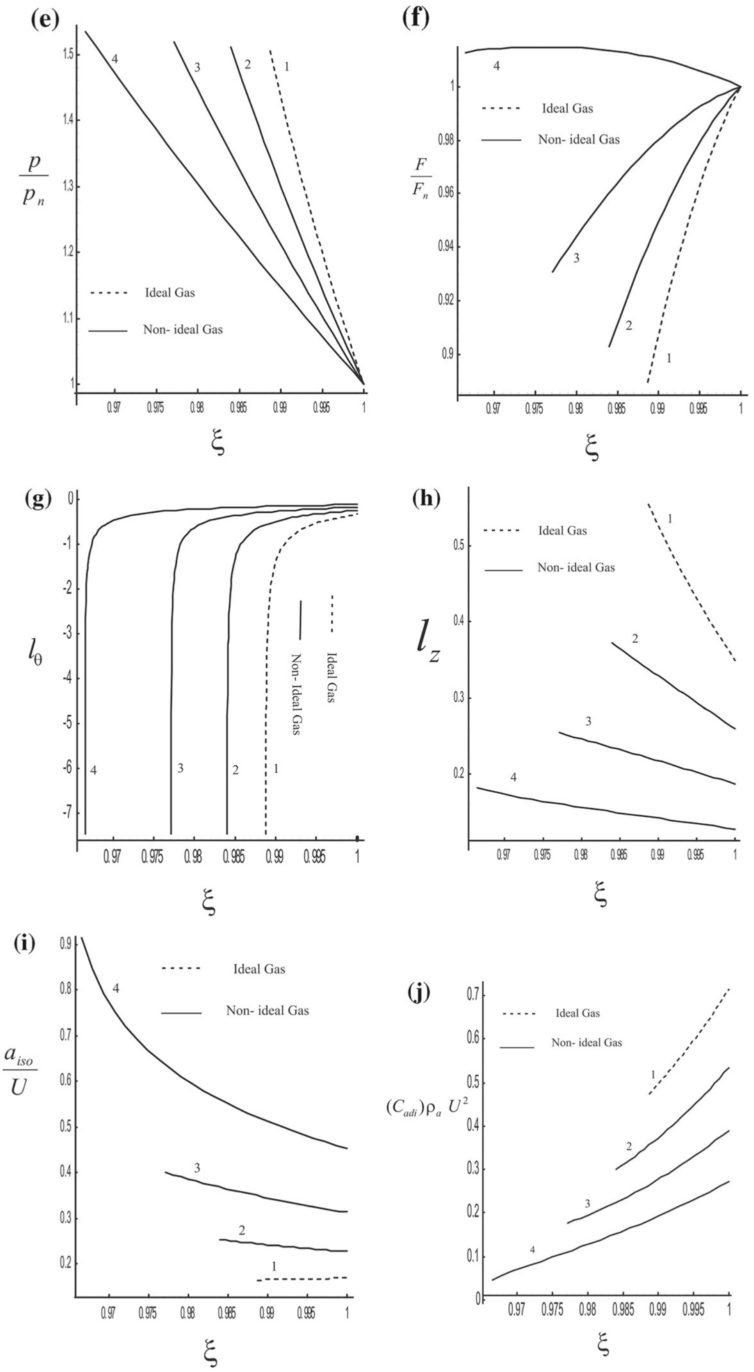

Fig. 2 continued

Table 1 The position of the piston ξ_p for different values of Γ_c with $\gamma = 1.4;\ \delta_c = 1;\ \delta_R = 2;\ M = 5;\ \overline{b} = 0.05,\ \Gamma_R = 10$

$\overline{b}$	β	Γ_c	Position of the piston ξ_p
0.05	0.0785714	1	0.988426
		1.5	0.982359
		2	0.976074
		3	0.966475
		3.5	0.965854
		10	0.963822
		∞	0.962855

Table 2 The position of the piston ξ_p for different values of Γ_R with $\gamma = 1.4;\ \delta_c = 1;\ \delta_R = 2;\ M = 5;\ \overline{b} = 0.05,\ \Gamma_c = 3$

$\overline{b}$	β	Γ_R	Position of the piston ξ_p
0.05	0.0785714	1	0.966479
		10	0.966475
		1000	0.966012
		5000	0.964922
		10000	0.964286
		15000	0.963946
		∞	0.962855

Table 3 The density ratio β across the shock and the position of the piston ξ_p for different values of $\overline{b}$ with $\gamma = 1.4;\ \delta_c = 1;\ \delta_R = 2;\ M = 5;\ \Gamma_c = 3,\ \Gamma_R = 10$

$\overline{b}$	β	$1-\beta$	Position of the piston ξ_p
0	0.0285714	0.9714286	0.988708
0.01	0.0385714	0.9614286	0.983983
0.025	0.0535714	0.9464286	0.977092
0.05	0.0785714	0.9214286	0.966475

From Table 1 and Fig. 1a–j it is found that the effects of an increase in the value of the conductive heat transfer parameter Γ_c are

(i) to decrease ξ_p, i.e. to increase the distance of the piston from the shock front. This means that an increase in the value of conductive heat transfer parameter has an effect of decreasing the shock strength i.e. the flow field behind the shock becomes somewhat rarefied (see Table 1);

(ii) to decrease the flow variables $\frac{u}{u_n}, \frac{\rho}{\rho_n}, \frac{p}{p_n}, \frac{F}{F_n}, l_z$ and $\frac{a_{isoth}}{U}$ at any point in the flow-field behind the shock front (see Fig. 1a, d–f, h, i);

(iii) to increase the flow variables $\frac{v}{v_n}, \frac{w}{w_n}, l_\theta$ and $C_{adi}\ \rho_a\ U^2$ at any point in the flow-field behind the shock front (see Fig. 1b, c, g, j).

Table 2 and Fig. 1a–j show that, the effects of an increase in the value of radiative heat transfer parameter Γ_R are similar to those of an increase in conductive heat transfer parameter Γ_c.

From Table 3 and Fig. 2a–j it is found that the effects of an increase in the value of the parameter of non-idealness of the gas $\overline{b}$ are

(i) to increase the value of β i.e. to decrease the shock strength (see Table 3);

(ii) to increase the distance of the piston from the shock front. Physically it means that the gas behind the shock is less compressed. This shows the same result as given in (i) above, i.e. there is a decrease in the shock strength (see Table 3);

(iii) to decrease the reduced radial component of fluid velocity $\frac{u}{u_n}$ near shock front but to increase it near piston (see Fig. 2a);

(iv) to increase the flow variables $\frac{v}{v_n}$, $\frac{w}{w_n}$, $\frac{F}{F_n}$, l_θ and $\frac{a_{isoth}}{U}$; whereas to decrease the flow variables $\frac{\rho}{\rho_n}$, $\frac{p}{p_n}$, l_z and $C_{adi}\ \rho_a\ U^2$ at any point in the flow-field behind the shock front (see Fig. 2b–j).

Conclusion

The present work investigates the unsteady adiabatic self-similar flow behind a exponential shock wave propagating in a rotational axisymmetric non-ideal gas with heat conduction and radiation heat flux. The density and angular velocity of the ambient medium are taken to be constants. The shock waves in rotational axisymmetric non-ideal gas with heat conduction and radiation heat flux can be important for description of shocks in supernova explosions, in the study of a flare produced shock in solar wind, central part of star burst galaxies, nuclear explosion, rupture of a pressurized vessel etc. On the basis of this work, one may draw the subsequent conclusions:

(i) An increase in the value of the parameter of conductive heat transfer Γ_c (or radiative heat transfer Γ_R) decreases the shock strength and widens the disturbed region between the shock and the piston.

(ii) An increase in the parameter of non-idealness of the gas has significant effects on the flow-variables between the shock and the piston. An increase in the value of the parameter of non-idealness of the gas and the conductive (or radiative) heat transfer parameter exhibits similar effects on the shock strength and on the distance between the shock front and the piston.

(iii) An increase in the value of conductive heat transfer parameter Γ_c (or radiative heat transfer parameter Γ_R) decrease the flow variables $\frac{u}{u_n}$, $\frac{\rho}{\rho_n}$, $\frac{p}{p_n}$, $\frac{F}{F_n}$, l_z, $\frac{a_{isoth}}{U}$; whereas reverse behaviour is observed in the case of the flow variables $\frac{v}{v_n}$, $\frac{w}{w_n}$, l_θ and $C_{adi}\ \rho_a\ U^2$.

(iv) An increase in the non-idealness of the gas $\overline{b}$ and the conductive heat transfer parameter Γ_c (or radiative heat transfer parameter Γ_R) have same behaviour on the flow variables $\frac{\rho}{\rho_n}$, $\frac{p}{p_n}$, $\frac{v}{v_n}$, $\frac{w}{w_n}$, l_θ and l_z; whereas opposite behaviour is observed in the case of flow variables $\frac{F}{F_n}$, $\frac{a_{isoth}}{U}$ and $C_{adi}\ \rho_a\ U^2$.

In this paper, the problem concerning the self-similar method for one-dimensional unsteady adiabatic flows behind an exponential shock wave with conductive and radiative heat fluxes in a rotational axisymmetric non-ideal gas is considered. Our considered problem consists of highly non-linear system of hyperbolic partial differential Eqs. (3)–(7). In order to find the solution of problem under consideration we employed the self-similarity method to transform the partial differential Eqs. (3)–(7) into ordinary differential Eqs. (39)–(44) and these equations are solved numerically by using Runge–Kutta method of fourth order. In the pioneer works (Igra et al. [30,31], Falcovitz et al. [32] and Falcovitz and Ben-Artzi [33]) the numerical solutions were compared with experimental finding and excellent agreement was found between the two, confirming the reliability of the numerical solution obtained for the considered problem.

In the present case the flow takes place in a non-ideal gas with conductive and radiative heat flux in rotating medium. Unfortunately, to the best of our knowledge there are no experimental results that can be used as a benchmark for the present problem. Also, to the best of our knowledge there are no research papers in literature for the shock wave problems by using homotopy perturbation method or variational iteration method [34,35] that can be used as benchmark for the considered flows. First of all one need to develop the correct formula for the correction functionals or to construct the homotopy for Eqs. (3)–(7) or (39)–(44) that is very interesting problem for future research.

References

1. Sedov, L.I.: Similarity and Dimensional Methods in Mechanics. Academic Press, New York (1959)
2. Marshak, R.E.: Effect of radiation on shock wave behavior. Phys. Fluids **1**, 24–29 (1958)
3. Elliott, L.A.: Similarity methods in radiation hydrodynamics. Proc. R. Soc. Lond. Ser. A **258**, 287–301 (1960)
4. Wang, K.C.: The piston problem with thermal radiation. J. Fluid Mech. **20**, 447–455 (1964)
5. Helliwell, J.B.: Self-similar piston problems with radiative heat transfer. J. Fluid Mech. **37**, 497–512 (1969)
6. NiCastro, J.R.: Similarity analysis of the radiative gas dynamic equations with spherical symmetry. Phys. Fluids **13**, 2000–2006 (1970)
7. Ghoneim, A.F., Kamel, M.M., Berger, S.A., Oppenheim, A.K.: Effect of internal heat transfer on the structure of self-similar blast waves. J. Fluid Mech. **117**, 473–491 (1982)
8. Chaturani, P.: Strong cylindrical shocks in a rotating gas. Appl. Sci. Res. **23**, 197–211 (1970)
9. Sakurai, A.: Propagation of spherical shock waves in stars. J. Fluid Mech. **1**, 436–453 (1956)
10. Nath, O., Ojha, S.N., Takhar, H.S.: Propagation of a shock wave in a rotating interplanetary atmosphere with increasing energy. J. Magnetohydrodyn. Plasma Res. **8**, 269–282 (1999)
11. Ganguly, A., Jana, M.: Propagation of shock wave in self-gravitating radiative magnetohydrodynamic non-uniform rotating atmosphere. Bull. Calcutta Math. Soc. **90**, 77–82 (1998)
12. Rao, M.P.R., Ramana, B.V.: Unsteady flow of a gas behind an exponential shock. J. Math. Phys. Sci. **10**, 465–476 (1976)
13. Anisimov, S.I., Spiner, O.M.: Motion of an almost ideal gas in the presence of a strong point explosion. J. Appl. Math. Mech. **36**, 883–887 (1972)
14. Rao, M.P.R., Purohit, N.K.: Self-similar piston problem in non-ideal gas. Int. J. Eng. Sci. **14**, 91–97 (1976)
15. Vishwakarma, J.P., Nath, G.: Similarity solutions for the flow behind an exponential shock in a non-ideal gas. Meccanica **42**, 331–339 (2007)
16. Nath, G.: Propagation of a cylindrical shock wave in a rotational axisymmetric isothermal flow of a non-ideal gas in magnetogasdynamics. Ain Shams Eng. J. **3**, 393–401 (2012)
17. Wu, C.C., Roberts, P.H.: Shock-wave propagation in a sonoluminescing gas bubble. Phys. Rev. Lett. **70**, 3424–3427 (1993)
18. Roberts, P.H., Wu, C.C.: Structure and stability of a spherical implosion. Phys. Lett. A **213**, 59–64 (1996)
19. Levin, V.A., Skopina, G.A.: Detonation wave propagation in rotational gas flows. J. Appl. Mech. Tech. Phys. **45**, 457–460 (2004)
20. Nath, G.: Magnetogasdynamic shock wave generated by a moving piston in a rotational axisymmetric isothermal flow of perfect gas with variable density. J. Adv. Space Res. **47**, 1463–1471 (2011)
21. Vishwakarma, J.P., Nath, G.: Similarity solutions for unsteady flow behind an exponential shock in a dusty gas. Phys. Scr. **74**, 493–498 (2006)
22. Gretler, W., Wehle, P.: Propagation of blast waves with exponential heat release and internal heat conduction and thermal radiation. Shock Waves **3**, 95–104 (1993)
23. Vishwakarma, J.P., Nath, G.: Propagation of shock waves in an exponential medium with heat conduction and radiation heat flux. Model. Meas. Control B **77**, 67–84 (2008)
24. Pomroning, G.C.: The Equations of Radiation Hydrodynamics, International Series of Monographs in Natural Philosophy, vol. 54. Pergaman Press, Oxford (1973)

25. Vishwakarma, J.P., Nath, G.: Similarity solution for a cylindrical shock wave in a rotational axisymmetric dusty gas with heat conduction and radiation heat flux. Commun. Nonlinear Sci. Numer. Simul. **17**, 154–169 (2012)
26. Laumbach, D.D., Probstein, R.F.: A point explosion in a cold exponential atmosphere. Part 2. Radiating flow. J. Fluid Mech. **40**, 833–858 (1970)
27. Nath, G.: Similarity solutions for unsteady flow behind an exponential shock in an axisymmetric rotating non-ideal gas. Meccanica **50**, 1701–1715 (2015)
28. Moelwyn-Hughes, E.A.: Physical Chemistry. Pergamon Press, London (1961)
29. Freeman, R.A., Craggs, J.D.: Shock waves from spark discharges. J. Phys. D **2**, 421–427 (1969)
30. Igra, O., Falcovitz, J., Reichenbach, H., Heilig, W.: Experimental and numerical study of the interaction between a planar shock wave and a square cavity. J. Fluid Mech. **313**, 105–130 (1996)
31. Igra, O., Wu, X., Falcovitz, J., Meguro, T., Takayama, K., Heilig, W.: Experimental and theoretical study of shock wave propagation through double-bend ducts. J. Fluid Mech. **437**, 255–282 (2001)
32. Falcovtiz, J., Alfandary, G., Ben-Dor, G.: Numerical simulation of the headon reflection of a regular reflection. Int. J. Numer. Methods Fluids **17**, 1055–1077 (1993)
33. Falcovitz, J., Ben-Artzi, M.: Recent developments of the GRP method. JSME Int. J. Ser. B. **38**, 497–517 (1995)
34. He, J.H.: Homotopy perturbation technique. Comput. Methods Appl. Mech. Eng. **178**, 257–262 (1999)
35. He, J.H.: Variational iteration method- a kind of non-linear analytical technique: some examples. Int. J. Non-linear Mech. **34**, 699–708 (1999)